Making MRI Quieter

William A. Edelstein[a], Robert A. Hedeen[a], Richard P. Mallozzi[a], Sayed-Amr El-Hamamsy[a,*],
Robert A. Ackermann[a], Timothy J. Havens[b]

[a]*GE Corporate R&D, Schenectady, NY, USA 12309*
[b]*GE Medical Systems, Florence, SC, USA 29501*

Abstract

We have mitigated acoustic noise in a 1.5 T cylindrical MRI scanner equipped with epoxy-potted, shielded gradients. It has been widely assumed that MRI acoustic noise comes overwhelmingly from vibrations of the gradient assembly. However, with vibration-isolated gradients contained in an airtight enclosure, we found the primary sources of acoustic noise to be eddy-current-induced vibrations of metal structures such as the cryostat inner bore and the rf body coil. We have elucidated the relative strengths of source-pathways of acoustic noise and assembled a reduced-acoustic-noise demonstration MRI system. This scanner employed a number of acoustic noise reduction measures including a vacuum enclosure of a vibrationally isolated gradient assembly, a low-eddy-current rf coil and a non-conducting inner bore cryostat. The demonstration scanner reduced, by about 20 dBA, the acoustic noise levels in the patient bore to 85 dBA and below for several typical noisy pulse sequences. The noise level standing near the patient bore is 71 dBA and below. We have applied Statistical Energy Analysis to develop a vibroacoustic model of the MR system. Our model includes vibrational sources and acoustic pathways to predict acoustic noise and provides a good spectral match above 400 Hz to experimentally measured sound levels. This tool enables us to factor acoustics into the design parameters of new MRI systems. © 2002 Elsevier Science Inc. All rights reserved.

Keywords: acoustics; noise; acoustic noise; MRI acoustic noise; sound

1. Introduction

Acoustic noise in MRI scanners has long been a concern for patient comfort and, on occasion, for patient safety [1,2]. Acoustic noise interferes with communication between MRI physicians and operators. Acoustic noise also provides an unwanted stimulus and interference during fMRI studies.

When we began our work, the standard GE product scanner had a heavy (~ 1000 kg) epoxy-potted shielded gradient supported on the cryostat via stiff aluminum brackets bolted to the bottom of the gradient assembly and the cryostat, one at each end of the magnet. In this configuration, fiberglass endcaps make a seal to the cryostat end flanges and to a cylindrical patient bore tube that surrounds the imaging subject. A whole-body birdcage rf coil, made of a large printed circuit board, is securely glued onto the outside of the patient bore tube. The endcaps, the cryostat flanges and inner bore, and the patient bore enclose the

gradient assembly. However, the endcaps have holes for airflow. Thus sound generated by the gradient coils could reach the patient bore or scan room via the endcap holes. Also, vibrations might be mechanically conveyed from the gradient assembly which could cause the cryostat or patient bore tube to vibrate and radiate sound.

We have studied acoustic noise in many modified configurations of this scanner. It has been widely assumed that acoustic noise comes directly from vibrations of the gradient assembly. However, when we vibrationally isolated the gradients in an airtight enclosure, we found that the primary sources of acoustic noise are eddy-current-induced vibrations of metal structures such as the cryostat inner bore and the rf body coil. We have elucidated the relative strengths of source-pathways of acoustic noise and assembled a "Quiet" reduced-acoustic-noise demonstration system. This scanner incorporates a variety of noise-reduction measures including a vacuum-enclosed, vibrationally isolated gradient assembly, a low-eddy-current rf coil and a non-conducting cryostat inner bore (NCCB). This Quiet scanner has reduced, by about 20 dBA from the standard scanner, the

* Corresponding author. Tel.: +1-518-461-6122.
E-mail address: wedelst1@nycap.rr.com (W.A. Edelstein)

acoustic noise levels in the patient bore to 85 dBA and below for several typical noisy pulse sequences. The noise levels for an operator standing outside the magnet bore are 71 dBA or below.

In previous work [3] we found that the gradient-to-noise acoustic transfer function is relatively flat above 700 Hz, with a myriad of peaks and valleys, but no overwhelming resonances. Below 700 Hz there is a substantial dropoff at low frequencies, which makes it possible to substantially decrease the noise output if MRI pulse sequences are tailored so that their high-frequency content is significantly decreased [4]. This can be accomplished by, for example, slowing down the rise and fall of the gradient pulses. However, this approach makes it difficult to implement fast pulse sequences, such as EPI or FSE, which require a large number of closely spaced gradient pulses. Our aim in this work has been to decrease sound levels without compromising scanner performance.

We have used the technique of SEA (Statistical Energy Analysis) [5] to create a vibroacoustic model of the MRI system. This model enables us to specify sources of vibration and the couplings between various structural and acoustic elements in order to characterize vibration and noise pathways. SEA model predictions are in good agreement with measured vibrations and sound levels at frequencies above 400 Hz.

2. Methods

Our goal is to reduce acoustic noise in the patient bore and in the vicinity of the magnet where operators or physicians may be positioned. Acoustic noise can be decreased either by reducing noise sources or by blocking pathways carrying the noise to the region of interest.

Toward this purpose we have investigated the *source-pathways* of acoustic noise. For each source there may be numerous pathways by which vibrations turn into sound heard by patient or scanner operator. A *source-pathway,* then, is a source together with a particular path for vibration transmission to the MRI system outer surface where the vibration radiates as sound. The outer surface includes the cryostat shell, the endcaps from magnet to patient bore tube and the patient bore tube.

For example, we have found that the conducting cryostat inner bore (CCB), driven by eddy current forces, is a major noise source. The two pathways for noise transmission from the CCB to the patient bore tube to the center of the patient volume are 1) the air between the CCB and the patient bore (in the gradient space) and 2) the mechanical pathway connecting the CCB to the outer surface. Hence one source-pathway is CCB through air to patient volume; another source-pathway is CCB via mechanical vibration to patient bore.

In order to find the hierarchy of source-pathways, we tried many different configurations of a 1.5 T cylindrical

scanner until changes were observed. Because of the logarithmic nature of sound perception, no clearly measurable alteration in sound level is obtained until one has an arrangement that affects the largest noise contribution. A loud noise masks a quieter one, so it is difficult to gauge the effect of changing a low-level noise source in the presence of a high-level source. In the present system, all noise is caused by and synchronized with the gradient pulses.

Suppose, for example, that one source-pathway delivers 95 dB of noise to the patient bore and another source-pathway produces 90 dB. The total noise is then 96.2 dB. Eliminating the quieter source-pathway will decrease the overall noise level by only 1.2 dB, which is close to the limits of perception, measurement and experimental reproducibility. Thus the effect of eliminating the quieter source-pathway is, for practical purposes, undetectable; progress can only be made by finding and affecting the loudest noise contributor.

To assess the effects of system changes, we used a suite of noisy pulse sequences with varying slice directions (axial, saggital, coronal) so that strong gradients would be applied along all three spatial directions. These pulse sequences were: FGRE, fast gradient recalled echo; SE, spin echo; FSPGR, fast spoiled grass; EPI-SE, echo-planar imaging, spin-echo; FSE, fast spin echo; FMPSPGR, fast multi-phase spoiled grass.

Many experiments were performed in order to isolate and identify noise sources and pathways. We applied and tested a large number of noise abatement measures, including vibration isolation, acoustic barriers and absorption, vacuum isolation, and constrained-layer damping. Once the major source-pathways were identified, we assembled a Quiet demonstration scanner that included all the noise abatement measures we had identified.

3. Experimental

We tested dozens of scanner configurations based on a standard LX-generation [6], 1.5 T GE product magnet (0.90 m inner cryostat bore diameter, 1.7 m bore length) equipped with imaging components including gradient and rf coils. This magnet has an electrically conducting, stainless steel inner cryostat bore (CCB, "conducting cryostat bore). In addition, a special magnet was made, identical to the standard LX product except that the CCB was replaced by a nonconducting, 3.8 mm thick fiberglass inner bore. Corresponding experiments were performed using this magnet.

In the standard GE MRI system, each end of the gradient assembly is attached to an aluminum bracket which, in turn, is solidly bolted to a second bracket fastened to the magnet cryostat. In order to provide vibration isolation between gradient assembly and cryostat, we decreased the thickness of both the gradient and magnet brackets and inserted three layers of 9.5 mm Isomode rubber in the space created. Isomode is a ribbed, low-durometer vibration isolation pad
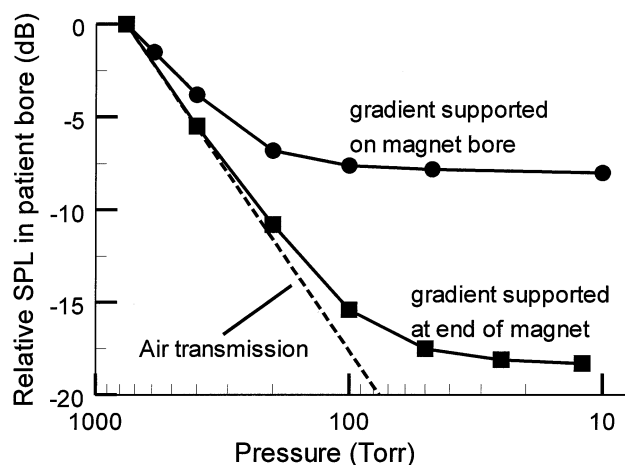
Fig. 1. Data showing *SPL* vs. *P* of an early model GE magnet having a gradient assembly with two different means of support. *SPL* initially follows the theoretical relationship $SPL \propto P^2$ but stops decreasing when the next loudest noise source-pathway manifests itself, in this case, the mechanical path from gradient assembly to patient bore. The upper curve corresponds to an arrangement where the gradient assembly was sitting on a rubber pad on the magnet bore. The lower curve corresponds to a configuration with an extended gradient assembly supported at the ends of the magnet.

commonly available from industrial supply outlets. We measured about 30 dB of mechanical vibration isolation between the magnet bracket and the gradient bracket.

Standard fiberglass endcaps going from magnet end flanges to patient bore were modified to form an airtight enclosure for the gradient assembly. Holes were covered and filled with fiberglass and the endcaps were reinforced with wood and fiberglass in order to withstand stresses created by evacuation of the gradient chamber.

The boundary of the airtight gradient chamber was thus the fiberglass patient bore, the endcaps and the cryostat inner bore. O-rings were used to make airtight seals from endcaps to patient bore and flat rubber gaskets sealed the endcaps to the cryostat end. One endcap was equipped with a vacuum fitting so that a vacuum pump could be attached.

The SPL (sound pressure level in decibels) of sound transmitted through a gas is proportional to the square of the pressure [9]: $SPL \propto P^2$. Therefore a tenfold pressure drop from 1 atm to 0.1 atm (760 Torr to 76 Torr) produces a 20 dB decrease in transmitted SPL, and a 100-fold drop to 7.6 Torr produces a 40 dB SPL decrease. These pressures do not require a high-quality vacuum system or expensive pumps.

In general, one observes an initial SPL decrease with the theoretical P^2 dependence and then the SPL decrease bottoms out when another noise source-pathway becomes evident. Fig. 1 shows SPL vs. P of an early model GE magnet (S-series, 0.95 m inner cryostat bore diameter, 2.2 m cryostat bore length) with two different means of gradient support. SPL initially follows the theoretical relationship $SPL \propto P^2$ but stops decreasing when the next loudest noise source-pathway manifests itself, in this case, the mechanical path from gradient assembly to patient bore. The upper curve

corresponds to a configuration where the gradient assembly is sitting on a rubber pad placed directly on the magnet bore. The lower curve was obtained when the gradient assembly was extended and supported on brackets at the ends of the magnet. The stiffer support provided more vibration isolation and weakened the gradient vibration to patient bore mechanical pathway.

Our experimental systems (based on the current model GE magnet) were capable of holding a vacuum with pressure below 10 torr under the best conditions, although 'vacuum' tests were generally performed at 25–100 torr. In all cases with low-pressure tests, we verified, by measuring sound output as a function of pressure, that the remaining air in the gradient space did not constitute a significant acoustic pathway.

Current feedthroughs for the gradient wires were made using 3/8″−16 studs that were bolted onto oversize holes with several layers of rubber washers. The rubber washers provided an airtight seal and a flexible connection to the endcaps so that Lorentz forces on the power cables (caused by pulsed gradient currents) would not be transmitted to the endcaps and generate sound-producing vibration. The product gradient wires were replaced by flexible welding cable with the same current-carrying capacity.

Acoustic noise levels were measured using two B&K Type 4189 prepolarized condenser microphones and B&K (Bruel and Kjaer Sound and Vibration, Copenhagen, Denmark, www.bksv.com/bksv) Type 2669 preamplifiers. One microphone was placed at the magnet isocenter (to measure sound that would be heard by an imaging subject) and the second was positioned in the room at a height of about 1.8 m, 3 m from the front of the scanner and 2 m to the side of the magnet centerline.

4. Results: Hierarchy of principal acoustic noise source-pathways

The standard product scanner has noise levels given in the two "Baseline" rows of Table 1. In this configuration, the endcaps are not sealed and the gradient coils are bolted directly to the magnet cryostat. Two principal source-pathways for noise to reach the center of the patient bore might be: gradient noise carried by air through holes in the endcaps; gradient vibrations conveyed mechanically, through the gradient support, which set up vibrations in the cryostat or patient bore and thereby generate sound.

As described above, to study individual source-pathways, the present series of experiments began after we first sealed the endcaps and installed vibration isolation for the gradient coils. The noise levels in this configuration were only slightly different from those in the standard scanner, and we did not specifically measure the separate source-pathways for the gradient assembly vibration isolation or holes in the standard scanner endcaps.

Table 1
Configurations and data for acoustic hierarchy determination

Test configuration	System components										Pulse sequence					
	Open end bells	Sealed end bells	Grads. bolted directly to cryostat	Grad. vibration isolation	Patient/ rf tube with live rf coil	Patient/ rf tube with no rf coil	1 Atm. pressure	Vacuum	Conduct-ing (metal) WB	Non-conducting (fiberglass) WB	FGRE	SE	FSPGR	EPI-SE	FSE	FMPSGR
											SPL (Sound pressure level) dBA					
Baseline1	•		•		•		•		•			99.0	105.0		97.0	106.0
Baseline2	•		•		•		•		•		94.0	100.0	106.0	94.5	96.5	107.5
A		•		•		•	•		•		96.5	95.5	96.0	98.5	95.0	103.5
B		•		•		•		•	•		87.0	89.5	89.5	94.0	85.0	90.5
C		•		•		•		•		•	81.5	85.0	86.0	83.0	81.5	83.0
D		•		•		•	•			•	85.5	88.5	88.0	86.5	96.0	89.5
E		•		•	•			•		•	91.0	96.0	93.5	92.0	94.0	101.5

The various contributions to the noise of the sealed, gradient-vibration-isolated scanner were determined by 'turning off' everything we could, measuring the 'background' level (i.e., all the sources we don't yet know how to turn off), then turning on the quietest source-pathway and measuring the difference. To get the other source-pathway contributions, we turned on each one while everything else was turned off. If that was not possible, we made sure at least to have everything off that was as loud or louder than the source-pathway of interest. By measuring the change in sound level when each source-pathway is switched on or off, we got a measurement of its contribution to the total sound energy S. Using this analysis, we could determine the acoustic power in each source-pathway and use the excess measurements to check for self-consistency.

Quantitation of the principal noise source-pathways was done using the data in Table 1 that shows variations of sound levels as a function of several scanner configurations and pulse sequences. The acoustic noise for any particular setup can have many contributions; however, as explained above, the loudest dominates. Eliminating or altering a source or pathway which does not affect the loudest noise may produce no change in sound level. Thus, necessarily, many experiments are carried out which do not substantially change the noise level and are not useful in helping to understand system noise. We have therefore selected in Table 1 a few scanner arrangements relevant to the hierarchy determination out of dozens of configurations tested.

To analyze the data in Table 1 we write the total sound energy S as the sum of source-pathways sound energies S_1, S_2, $S_3 \ldots$

$$S = 10 \cdot \log(10^{(S_1/10)} + 10^{(S_2/10)} + 10^{(S_3/10)} + \ldots) \quad (1)$$

where the energies are all measured in dB. The data in Table 1 for Test Configurations A-E are expressed as systems of equations of the form Eq. 1 and then solved for individual SPL contributions. The results are shown in Fig. 2.

By this process we identified two dominant sources of acoustic noise in the sealed, gradient-vibration-isolated MRI system: eddy-current-induced vibrations of the metal, electrically conducting cryostat bore (CCB); and eddy-current-induced vibrations of the rf coil mounted on the patient tube. These two sources are typically 10–15 dB more powerful than any other lesser source in the system. They produce roughly equal magnitudes of acoustic noise. Interestingly (and contrary to expectations), noise from the gradients transmitted directly through air is not one of the major source-pathways for acoustic noise in our system once the gradients are vibrationally isolated and contained in an airtight enclosure with no acoustic "leaks."

Also shown in Fig. 2 are the noise levels of the 'remainder,' which consists of all sources and pathways that we
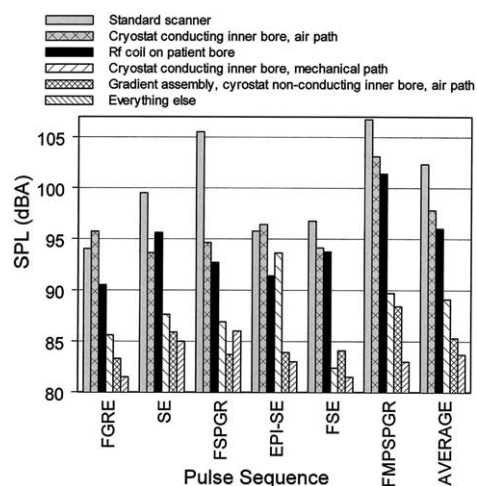

Fig. 2. Acoustic noise levels, in the patient bore, for a standard MRI scanner and for individual source-pathways for several MRI pulse sequences in a modified scanner. The standard scanner has the gradient assembly bolted directly to the magnet cryostat and the endcaps between cryostat and patient bore have holes through which sound can travel. The modified scanner has a vibration-isolated gradient assembly and sealed endcaps. The loudest source-pathways are electrically conducting cryostat bore (CCB) transmitted through air and the rf coil on the patient bore.

have not yet broken down or understood. Leading candidates for 'remainder' source-pathways are eddy-current-induced vibrations of the magnet interior, cryostat flanges or outer cylinder; and residual mechanical vibrations of the gradients that may be getting through the vibration isolation pads. Further experiments are necessary to determine which (if any) of these sources dominate the remaining noise.

One mechanism by which the CCB might be producing acoustic noise in the patient bore is a "drum" effect, that is, motion of the CCB changes the pressure in the gradient chamber and consequently moves the patient bore. This is what happens in a drum with two stretched skins: displacement of the bottom skin causes the top one to move. In this regard it is interesting to note that, for FGRE and EPI-SE, the standard scanner noise levels are actually slightly lower than the CCB source-pathway via air. So it is plausible that completely sealing the gradient chamber has increased the acoustic noise-generating effect of CCB motion because of the drum effect.

In summary, the major acoustic noise source-pathways to the patient, in order of strength, are as follows.

Standard imager
1. Lorentz forces acting on the gradient coils transmitted via air through holes in the endcaps or as vibration through the gradient supports into the MRI structure.

Imager with sealed endcaps and vibration-isolated gradients
2. Eddy-current-induced vibrations of a metallic, conducting cryostat inner bore (CCB). The path in this case may be either sound radiated directly from the CCB or movement of the patient tube because the CCB and patient tube are the thinnest boundaries of the sealed gradient chamber. (The latter mechanism is similar to pushing in one side of a drum and having the other side bulge.)
3. Eddy-current-induced vibrations of the rf body coil mounted on the rf/patient tube radiating sound to the imaging subject.
4. Eddy-current-induced vibrations of the CCB transmitted by mechanical means to the rf/patient tube.
5. Gradient assembly vibrations radiating sound through air in the gradient space plus cryostat vibrations radiating sound or mechanically transmitting vibrations to the rf/patient bore.
6. Remaining, unknown source-pathways possibly including noise generated by vibrations mechanically transmitted through the gradient vibration isolation.

5. QUIET DEMONSTRATION SCANNER

Using all noise abatement measures we could muster, we assembled a noise-reduced "Quiet" scanner that achieved an acoustic noise reduction of 22 dBA in the patient bore and 20 dBA in the scan room. (These figures represent the change from the loudest of five test pulse sequences in the standard product to the loudest test pulse sequence in the

Fig. 3. Standard rf body coil (A) and low-eddy-current (LEC) rf coil (B) constructed for the Quiet Demonstration scanner. The standard rf coil pattern is etched and supported by a sheet of plastic that is glued onto the outside of the patient tube. Eddy currents generated in the ~5 cm wide copper strips by the pulsed gradients interact with the static magnetic field, exert Lorentz forces on the patient tube and produce acoustic noise. The longitudinal runs of the LEC coil are made from 6.4 mm OD Cu tubing, and the tubing plus endrings are supported on a thin layer of soft rubber running circumferentially around the patient tube.

Quiet scanner.) All five test pulse sequences yielded noise below 85 dBA at the patient bore isocenter and below 70.5 dBA in the scan room. In addition to the non-conducting cryostat inner bore (NCCB), a number of other measures were applied to achieve noise abatement, most notably an "LEC" (low-eddy-current) rf coil, constrained-layer damping on the patient bore, low-eddy-current passive magnet shims, acoustic absorption in the bore and acoustic barrier material on the outside of the magnet cryostat.

5.1. LEC body birdcage coil

As shown in Fig. 3A, the standard GE rf body birdcage coil uses an etched printed circuit form with 5 cm wide copper runs. These conductors are very close (less than 20 mm) to the inside of the gradient assembly and are therefore subject to intense pulsed gradient fields. The pulsed fields create eddy currents in the conductors, and these currents interact with the 1.5 T static magnetic field to impose strong Lorentz forces on the conductors. The patient tube is forced to vibrate and radiate acoustic noise to the imaging subject.

The LEC rf body birdcage coil (Fig. 3B) uses 6.4 mm OD Cu tubing in place of the 5 cm wide strips of the product coil. The area subject to pulsed gradient fields is reduced.

Therefore the eddy currents are smaller as are the Lorentz forces, consequent vibration and acoustic noise. Further, the Cu tubing is supported on a 1.6 mm thick layer of Neoprene that decreases the transmission to the patient tube of any vibrations created in the rf coil.

Other strategies to reduce the acoustic contribution of the rf body coil are to remove the rf coil from the patient bore surface altogether [7] or use capacitive coupling to interrupt induced eddy currents while allowing the flow of rf currents [8].

5.2. Non-conducting passive magnetic shims

Passive magnetic shims attached to the inside of the cryostat inner bore also contribute to the scanner acoustic noise. These shims ordinarily consist of 3-cm-wide strips of magnetic stainless steel glued to the cryostat inner bore. However, because they are electrically conducting, these shims support eddy currents driven by the gradient fields that leak out of the gradient assembly and therefore are subject to Lorentz forces that can vibrate the cryostat inner bore. In the above discussion and in Fig. 2, we have lumped the shim contribution in with the conducting cryostat inner bore contribution. By studying the measurements more carefully, we infer that the shim contribution to noise is small compared to that of the conducting cryostat inner bore. We deduce that noise levels from metallic, conducting shims on our NCCB are close to 88–89 dBA for the louder pulse sequences.

In the Quiet demonstration scanner we used LEC (low-eddy-current) shims made by mixing 100 mesh steel powder into epoxy. The bulk material was then molded in a high-temperature press, removed and cut into strips. The strips were then pressed to final thickness and trimmed to the desired length and width. Shim stock was made in five different thicknesses, 0.25 mm to 1.25 mm in 0.25 mm increments. Since shimming is typically performed by iron weight measurements, the amount of iron was derated by the ratio of iron density to effective density, i.e., $\rho_{Fe}/\rho_{eff} = 1.79$.

Electrical resistance of normal iron shims is a fraction of an ohm, whereas the resistance of these shims was in the range of 100 Ω to 1 kΩ. This should not support appreciable eddy currents. To test this possibility, shim strips were mounted on a fiberglass cylinder and introduced into a magnet while applying strong gradient field pulses perpendicular to the plane of the strips, and the motion was monitored by accelerometers. No discernable vibrational forces were detected.

5.3. Constrained-layer damping

CLD (constrained-layer damping) was installed on the outside of the magnet cryostat and the inside of the patient tube. Our CLD consisted of a thin sheet of flexible, solid material attached, by a lossy elastomer, to a surface that may have acoustic resonances. In this case we used thin (0.5

Table 2
MRI quiet demonstration noise levels (dBA)

	Standard system		Quiet demo system	
	Cryostat bore	Room	Cryostat bore	Room
FGRE	94	87	82	68.5
SE	100	93.5	79	69.5
FSPGR	106	93	84	70.5
EPI-SE	94.5	92	78.5	68
FSE	96.5	90	80.5	67.5
FMPSPGR	107.5	98.5	81	68

mm) fiberglass sheet and 3M sticky film (Scotch 924 Adhesive Transfer Tape). As the object surface flexes because of vibration, strain is created between the original surface and the CLD solid sheet, and the intermediate elastomer absorbs energy. Thus the effect of CLD generally is to introduce mechanical damping and thereby reduce the amplitude of resonant peaks in the acoustic spectrum that would otherwise raise the overall noise level. The CLD in the present case reduced the noise level by 1–2 dBA.

5.4. Sound barrier materials

1.5 lb/ft^2 (72 Pa) "Soundmat" (Soundcoat Co., Deer Park, NY, www.soundcoat.com) was applied to the outside of the cryostat. This material has an outer layer of 3.2 mm thick mass-loaded vinyl bonded to a layer of 6.4 mm thick Soundfoam. It has an adhesive backing and was applied foam side in. In this case, the foam provided little if any acoustic absorption, but served to decouple the barrier layer from the vibrating magnet vessel. It provided approximately 5 dBA noise level reduction in the imager room.

12.7 mm thick "Soundfoam" sound absorber material (Soundcoat Co.) was placed on the patient couch. This material is open-cell polyurethane foam. It has a white matte finish and surface barrier that is impervious to dirt, grease and chemicals. It has an adhesive backing and was applied by pressing it onto the patient couch after removing protective paper backing. The purpose of the Soundfoam absorber is to absorb sound in the patient volume, especially sound that might build up because of "organ pipe" resonances of the patient cavity. For the same reason, we also placed about 0.9 m^2 of 25.4 mm thick Soundfoam, with no covering skin, in cavities beneath the patient bridge. The Soundfoam produces approximately 1–2 dBA noise reduction in the patient bore.

5.5. Quiet demonstration scanner noise levels

Table 2 shows the noise levels achieved in the Quiet Demonstration scanner for our six test pulse sequences compared to the same six sequences in the standard GE MRI system. The noise levels in the "interventional" position (doctor or technician standing at the mouth of the magnet) are about 2 dBA louder than the room acoustic

levels. At that level (≤73 dBA) it is possible to carry out a conversation in a normal voice.

5.6. Next quiet measures?

It is interesting to ask how further reductions could be achieved, i.e., what are the next loudest source-pathways and how can they be defeated. One possibility is that vibrations from the gradient assembly, although reduced by 30 dB by the vibration isolation, may vibrate the system enough to produce the sound remaining when other measures described above have been applied. This might be mitigated by supporting the gradient assembly directly from the floor [10].

6. Acoustic modeling

In order to further understand the physical production and transport of vibration and noise, we developed a vibro-acoustic model of our Quiet Demonstration scanner using Statistical Energy Analysis (SEA) [5]. At frequencies such that system structures have a high density of vibrational modes and energy is roughly equipartitioned among these modes, the flow of vibrational energy from one structure to another is proportional to the difference between average modal energies in, and coupling between, the two structures. This is the basis of SEA.

In a system the size and structure of an MRI scanner, this happens at frequencies above about 400 Hz. Many MRI scan sequences contain a short gradient pulse pattern which is regularly repeated every 10 ms or so. The consequent acoustic noise comprises harmonics of the repetition frequency (~100 Hz) with harmonic components extending beyond 5 kHz, and the majority of MR vibroacoustic energy falls into an SEA-valid range [3]. The high frequency content of the noise, the simple, lightly damped structure, and the structural-acoustic interactions involved make MRI scanners well suited to SEA analysis.

Application of SEA principles allows us to reduce a complicated vibration problem to a simpler energy balance problem similar to classic conductive heat transfer. A physical model is developed consisting of subsystems, which can be solid structures or acoustic spaces, and junctions between the subsystems. Sources of vibrating mechanical power, which excite the system, are determined by a combination of physical analysis and experiment and applied to the model. The vibratory energy flows between groups of similar response modes in adjacent subsystems, the rate of flow being proportional to the difference of modal energy in the subsystems and to the internal losses in the junctions between them. The resulting steady state energy levels of the model subsystems are calculated, and then converted to the physical response of each subsystem in terms of acceleration or sound pressure. The analysis and results are performed in terms of an average over each frequency band
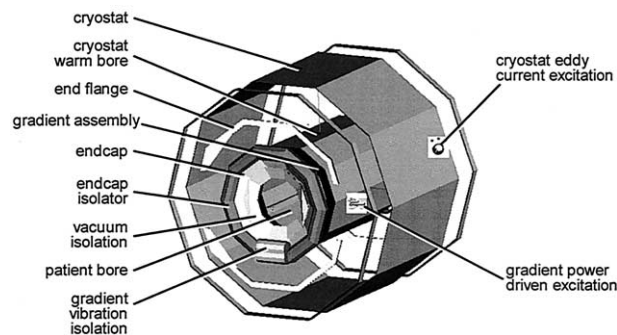

Fig. 4. Schematic MRI system as used by SEA (Statistical Energy Analysis) software. The gradient assembly is supported by the cryostat via rubber vibration isolation. The gradient assembly is enclosed in an airtight chamber bounded by the magnet inner bore, the patient tube and airtight fiberglass endcaps. The gradient assembly chamber can be pumped down to a pressure of about 10 Torr. Excitations include: Lorentz-forces acting on the gradient coil; and Lorentz forces on the cryostat inner bore because of pulsed-gradient-field induced eddy currents. The SEA model provides vibrational modes for the various subsystems and coupling coefficients between subsystems.

and subsystem. This limits the resulting detail, but knowledge of the average and variance of the system response is usually adequate for assessment of designs and modifications. SEA also avoids the high computational cost and often misleading detail of more deterministic approaches such as finite element analysis.

We used a commercially available SEA code known as AutoSEA (Vibroacoustic Sciences, Inc., San Diego CA, USA). Per usual SEA procedures, the MRI scanner model (Fig. 4) is built up with geometrically simple subsystem elements such as plates, cylinders, isolators, acoustic cavities, etc. Physical detail smaller than an acoustic wavelength is not required in this analysis. Basic physical properties of the subsystems, such as density, modulus, and damping are associated with each subsystem. Junctions between adjacent subsystems include coupling loss factors, which determine the "resistance" to energy flow between subsystems. The coupling loss factors are determined from either basic principles or experimental measurements and are applied to the model. For example, the scanner endbell is a subsystem consisting of a cone of laid-up fiberglass epoxy. The junction between the fiberglass end bell and the cryostat steel end flange is given the properties (modulus, density, etc.) of Butyl rubber to simulate the vibration isolating rubber gasket we used. The endbell also shares a hard mounted junction with the fiberglass patient bore, the end flange is welded at a 90° angle to the cylindrical steel cryostat shell, and so on.

Input power to the system was due to two mechanisms. Very large Lorentz forces $B_0 \times I$ in the gradient coils are the prime system excitation. (B_0 is the static magnetic imaging field, 1.5 T in the present example, and I is the current through an individual wire in the gradient assembly, typically 200 A or more.) Spectral values of this excitation were obtained by direct measurement of gradient vibration. Be-

cause of high electromagnetic fields produced by the gradient, Lorentz forces caused by eddy currents in electrically conducting structures near the gradient also introduce sources of vibratory power. The eddy-current-induced forces in the cryostat inner bore and end flanges were calculated by a separate analysis.

Our system SEA model consists of a total of 28 subsystems and 53 junctions. Solution of the main energy-coupling matrix is efficient and takes only about 5 min on a 266 MHz, Pentium-II laptop computer. Subsequent runs on minor model modifications are completed in less than a minute each. We were primarily interested in the sound pressure of the patient bore acoustic volume subsystem. We also calculated the vibration spectra of other parts of the scanner as well as sound pressure in the surrounding test room.

7. Comparison of sea model results and measurements

We rely on experimental observations of our experimental scanner for some of the driving excitations and for validation of the results of the analysis. Experimental scanner features incorporated into the model include elastomeric vibration isolators on the gradient coil and the patient bore tube, a sealed vacuum compartment surrounding the gradient, a cryostat inner bore made of fiberglass rather than the standard stainless steel, and an RF coil mechanically isolated from the patient bore tube. We chose a particularly noisy standard scan sequence, FMPSPGR, to evaluate with our SEA model. During the scan, we used small accelerometers to measure the vibration of the structural subsystems and well-shielded instrumentation grade microphones to monitor acoustic subsystems. The frequency content of the data signals is obtained by digital octave filters.

Figs. 5 and 6 show modeled and measured response spectra for the two subsystems of greatest practical interest, the patient bore vibration and the sound pressure level inside the patient bore. The spectra agree well, especially at frequencies above 400 Hz where the SEA technique is most valid for this system. The A-weighted overall sound pressure levels, modeled and measured, agree to better than 2 dBA.

8. Conclusions

Finding the fundamental causes of acoustic noise in MRI systems is difficult because of the diffuse nature and logarithmic perception of sound. Experiments involve changing major portions of the scanner and require substantial engineering resources. We have found high levels of acoustic noise generated by Lorentz forces on gradient-induced eddy currents in some metallic portions of the scanner, specifically the rf body coil mounted on the patient bore and the
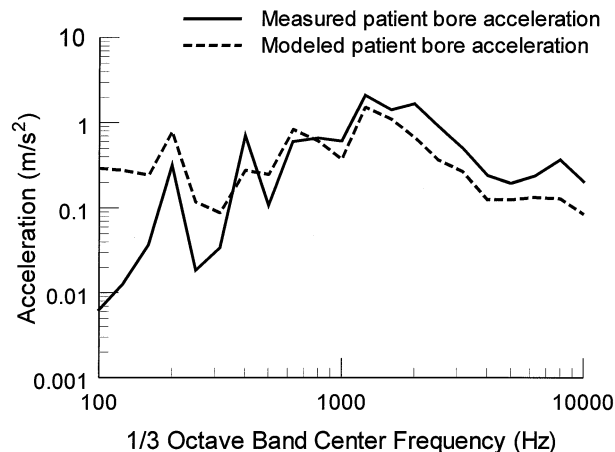

Fig. 5. Patient bore acceleration modeled (SEA) and measured (accelerometers) for MRI pulse sequence FMPSPGR. The two spectra agree well above 400 Hz where SEA is applicable for this system.

metallic inner bore of the magnet cryostat. In order to find and eliminate yet lower noise contributions, we may need to look for acoustic eddy current effects in other metallic parts of the scanner, and additionally try to mitigate vibrations that may be transmitted to the patient bore through the gradient assembly vibration isolation. It is also conceivable that the eddy currents could be reduced through better-shielded gradient designs. Using experimental results and calculations as input, the SEA vibroacoustic approach yields a reasonably accurate description of the MRI system and gives hope that acoustic noise can be included as a quantifiable design goal in MRI. The simplicity of the SEA model and the speed of its solution allows rapid evaluation of the effect of changes in structure, material, or scan sequence on the patient's noise exposure. Further scanner
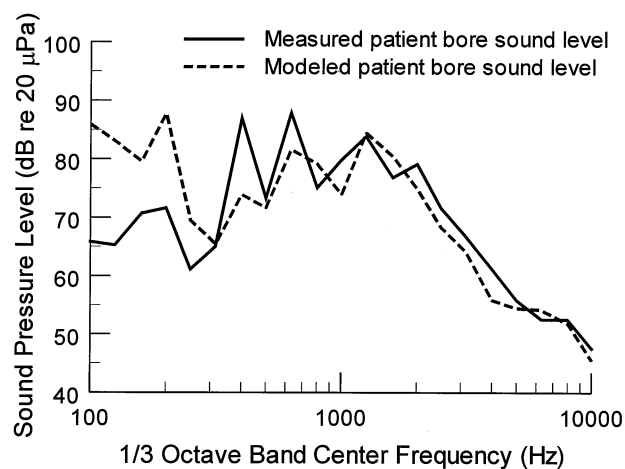

Fig. 6. Patient bore SPL modeled (SEA) and measured (microphone) for MRI pulse sequence FMPSPGR. The two spectra agree well above 400 Hz where SEA is applicable for this system. The overall A-weighted SPLs, modeled and measured, agree to better than 2 dBA.

noise reduction work is utilizing the output of the model prediction to find the next levels of sound production.

Acknowledgments

References

[1] Quirk ME, et al. Anxiety in patients undergoing MR imaging. Radiology 1989;170:463–6.

[2] McJury MJ. Acoustic noise levels generated during high field MR imaging. Clinical Radiology 1995;50:331–4.

[3] Hedeen RA, Edelstein WA. Characterization and prediction of gradient acoustic noise in MR imagers. Magnetic Resonance in Medicine 1997;37:7–10.

[4] Hennel F, Girard F, Loenneker T. 'Silent' MRI with soft gradient pulses. Magnetic Resonance in Medicine 1999;42:6–10.

[5] Lyon RH, DeJong RG. Theory and Application of Statistical Energy Analysis, second edition, Butterworth-Heinemann, 1995, ISBN 0–7506-9111–5

[6] Ackermann RA, Herd KG, Chen WE. Advanced cryocooler cooling for MRI systems. In: Ross RG, editor. Cryocoolers 10. New York: Plenum, 1999. p. 857–67.

[7] Purgill DA, Radziun MJ, Dean DE. Reduced Noise Rf Coil Apparatus for MR Imaging System. US Patent 6,252,404 (6/26/2001, priority 7/18/1999).

[8] Weyers DJ, Li S, Dean DE. RF Birdcage Coil with Reduced Acoustic Noise. Patent Pending.

[9] Kinsler LE, Frey AR. Fundamentals of Acoustics. 2nd edition. New York: John Wiley and Sons, 1962.

[10] Iinuma K, Katsunuma A, Kawamoto H, Takamori H, Toyoshima T, Uosaki Y, Yamagata H, "Magnetic resonance imaging system having mechanically decoupled field generators to reduce ambient acoustic noise," US Patent 6,043,653, (March 28, 2000).